

# Hexagonal AlN (0001) heteroepitaxial growth on cubic diamond (001)

Kazuyuki Hirama<sup>1</sup>, Yoshitaka Taniyasu<sup>1</sup> and Makoto Kasu<sup>1</sup>

<sup>1</sup> NTT Basic Research Laboratories, NTT Corporation  
3-1, Morinosato Wakamiya Atsugi-shi, Kanagawa 243-0198 Japan  
Phone: +81-46-240-3356 E-mail: k.hirama@will.brl.ntt.co.jp

## 1. Introduction

The aluminum nitride (AlN)/diamond heterostructure is expected to open a new way to achieve hybrid nitride and diamond devices. For nitride high-power devices, AlN on diamond substrate is an effective template for improving heat spreading from the devices because diamond has the highest thermal conductivity (22 W/cm K) among materials. For diamond high-power transistors, an n-type AlN/diamond heterostructure could be used for modulation doping because the bandgap of AlN (6 eV) is larger than that of diamond (5.47 eV) and an n-type doping is possible for AlN. Furthermore, an n-type AlN/p-type diamond heterojunction is one approach toward deep ultraviolet light-emitting diodes (LEDs). However, AlN has a hexagonal (wurtzite) crystal structure while diamond has a cubic (diamond) crystal structure. By using (111) surface orientation to overcome the difficulties due to the different crystal structures, we obtained single-crystal AlN (0001) layers grown on diamond substrates [1].

On the other hand, diamond (001) is preferred to diamond (111) because the mobility on (001) ( $>1300 \text{ cm}^2/\text{Vs}$ ) [2] is higher than that on (111) ( $\sim 800 \text{ cm}^2/\text{Vs}$ ). Actually, the RF cut-off frequency of diamond FETs is higher for (001) [3]. In (111) diamond growth, twinning easily occurs because stacking faults are introduced [4].

Vogg *et al.* have reported AlN layer growth on diamond (001) and the formation of rotated domains [5]. However, the formation mechanism of the AlN domain structures is not clearly understood yet. In this work, to understand the mechanism of heteroepitaxial growth of AlN on diamond (001), we investigated the structural properties of the AlN layers on diamond (001).

## 2. Experimental

Undoped 0.5- $\mu\text{m}$ -thick AlN layers were grown on high-pressure and high-temperature synthesized Ib-type diamond (001) substrate by low-pressure MOVPE. The source gases were trimethylaluminum (TMA) and ammonia ( $\text{NH}_3$ ). The carrier gas was purified (9N) hydrogen ( $\text{H}_2$ ). Before AlN growth, thermal cleaning was performed in  $\text{H}_2$  atmosphere for 10 min. The cleaning and growth temperature were the same, 1200 °C. At the growth temperature, the growth rate was 0.5  $\mu\text{m}/\text{h}$ .

In the X-ray diffraction (XRD) pole figure measurements of the AlN layers on the diamond (001) substrate, the directions of  $\Phi = 0^\circ$  and  $\Psi = 0^\circ$  were defined as the diamond [1-10] and [001] directions, respectively.

Cross-sectional TEM images of the AlN/diamond hetero-interface were taken along the diamond [1-10] zone axis, and the projection was the diamond [110] axis.

## 3. Results and discussion

### 3.1 Domain structure of AlN on diamond (001)

Figure 1(a) shows the pole figure of the AlN (0002) plane on diamond (001). A strong peak was observed at  $\Psi = 0^\circ$ . This indicates that AlN (0001) was mainly epitaxially grown on diamond (001). In addition, four weak diffraction peaks were observed at  $\Psi = 55^\circ$ , indicating the existence of the tilted domains. Figure 1(b) shows the pole figure of the AlN (10-11) plane. Twelve diffraction peaks were observed at  $\Psi = 61.6^\circ$ . In principle, a single domain should have six peaks. This indicates the formation of rotated domains with in-plane orientations rotated by  $30^\circ$  with respect to each other.

### 3.2 Tilted AlN domains on diamond (001)

Figure 2(a) shows a TEM image of the tilted AlN domains on diamond (001). As shown in the image, the [0001] direction of the tilted AlN domains was inclined at  $55^\circ$  from the diamond [001] direction, and the tilted domains nucleated on the facets of the pits that formed on the diamond surface. Because the facet angle from the diamond (001) surface corresponds to the angle between diamond (001) and (111) ( $54.7^\circ$ ), the facet of the pits is found to be the {111} face. These results agree with the XRD pole figure [Fig.1 (a)].

Before the thermal cleaning process in  $\text{H}_2$  gas, no pits were observed on the (001) substrate. Therefore, we con-

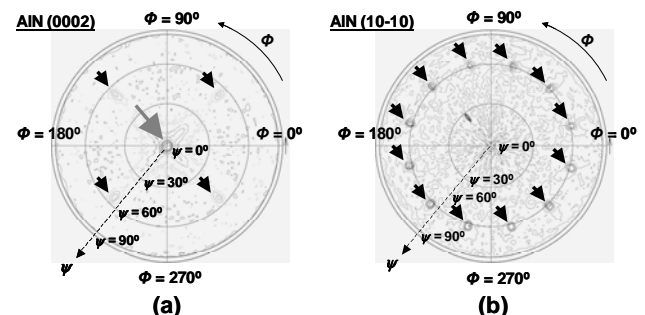


Fig. 1. XRD pole figures of (a) AlN (0002) and (b) AlN (10-11) planes of AlN layers on diamond (001). The directions of  $\Phi = 0^\circ$  and  $\Psi = 0^\circ$  were set to the diamond [1-10] and [001] directions, respectively. (a) A large arrow indicates the diffraction peak from the predominant domain with the c-axis parallel to the diamond [001] direction. Four small arrows indicate the tilted domains. (b) Twelve arrows indicate the existence of rotated domains.

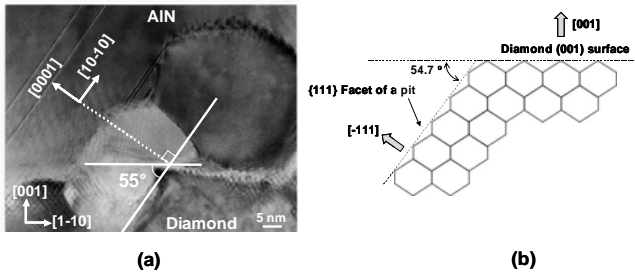


Fig. 2. (a) Cross-sectional TEM images of AlN/diamond interfaces with tilted domains on diamond (001). (b) Relationship between the diamond (001) surface and pits with {111} facets.

sider that during the thermal cleaning process in  $H_2$  gas, the diamond (001) surface is partially etched, and the pits with {111} facets are generated. On the other hand, no pits were observed on the (111) substrate after the same thermal cleaning process because the (111) diamond surface is more stable than the (001) diamond surface.

One possible mechanism of pit formation on diamond (001) substrate is the transformation of diamond into graphite and the subsequent etching of the graphite at high temperature in  $H_2$  atmosphere. Although the diamond surface is stable below  $1600^\circ C$ , its transformation into graphite occurs at lower temperature if chemical reagents (such as defects or catalytically active metals) exist near the surface [6]. Therefore, the graphite would be etched before the AlN growth and pits would then form on the diamond (001) surface. Another possibility is that residual oxygen or  $NH_3$  gas in MOVPE reactor etches the diamond surface.

### 3.3 Rotated AlN domain on diamond (001)

Figure 3(a) shows a TEM image of rotated AlN domains on the diamond (001) substrate. We found that the rotated domains started to form just on the diamond surface; they did not form during AlN growth. In this image, on the left side, the AlN [11-20] direction aligns to diamond [1-10], while on the right side, the AlN [10-10] direction aligns to diamond [1-10].

Figure 3(b) shows the schematic top and cross-sectional views of AlN (0001) layers on diamond (001) surfaces. With annealing at over  $1000^\circ C$ , a diamond (001) surface forms  $\pi$ -bonded structures and a reconstruction occurs with a C-C dimer [7]. On every atomic layer, the direction of the dimer rotates by  $90^\circ$ ; its direction changes between [1-10] and [110] [8]. Therefore, if AlN nucleates on two different reconstructed (001) terraces, the AlN domains are rotated on diamond (001) by  $30^\circ$  with respect to each other. This is consistent with the two different rotated domains in Fig. 1(b).

### 4. Summary

We achieved AlN (0001) heteroepitaxial growth on diamond (001) and clarified the mechanism of epitaxial growth of AlN layers on diamond (001). From XRD and TEM, we found tilted and rotated domains in AlN, which are directly nucleated on diamond (001) surface. The tilted

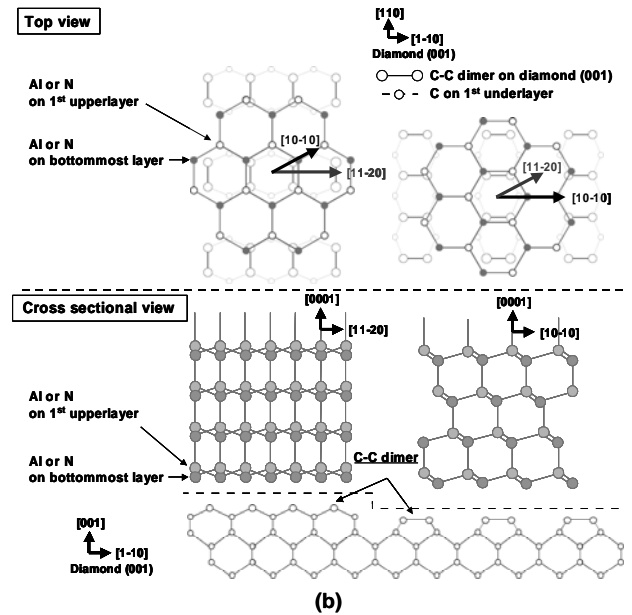
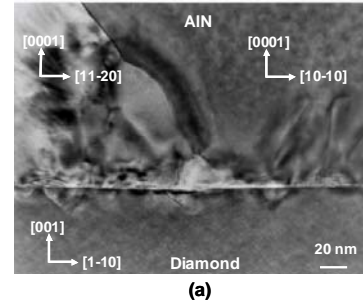


Fig. 3 (a) Cross-sectional TEM images of the AlN/diamond interface with rotated domains on diamond (001). (b) Schematic top and cross-sectional views of the rotated domains on diamond (001).

domains form on the {111} facets of the pits created during the thermal cleaning process in  $H_2$  and the rotated domains form due to the two different crystallographic symmetries of the AlN (0001) and diamond (001) surfaces.

### Acknowledgements

This work was partly supported by the SCOPE project.

### Reference

- [1] Y. Taniyasu, M. Kasu, J. Cryst. Growth, (2009) online available.
- [2] M. Kasu, N. Kobayashi, Appl. Phys. Lett., 80 (2002) 3961.
- [3] M. Kasu, K. Ueda, H. Ye, Y. Yamauchi, S. Sasaki, T. Makimoto, Electron. Lett. 41 (2005) 1249.
- [4] M. Kasu, T. Makimoto, W. Ebert, E. Kohn, Appl. Phys. Lett., 83 (2003) 3465.
- [5] G. Vogg, C.R. Miskys, J.A. Garrido, M. Hermann, M. Eickhoff, M. Stutzmann, J. Appl. Phys. 96 (2004) 895.
- [6] B. Pate, "Diamond surface", in "Diamond: Electronic Properties and Applications", Kluwer Academic Publishers, (1995) p36.
- [7] R.E Thomas, R.A. Rudder, R.J. Markunas, J. Vac. Sci. Technol. A, 10 (1992) 2451.
- [8] K. Yalai, W. Yafei, L. Naeson, B. Andrzej, B. Teresa, T. Tien, Appl. Phys. Lett., 67 (1995) 3721.